ION IMPLANTED OBLIQUE INCIDENCE MAGNETOSTATIC WAVES

F-3

R. L. Carter, J. M. Owens, C. V. Smith, and K. W. Reed

The University of Texas at Arlington 76019

ABSTRACT

Ion implanted bars have been used in MSFVW oblique incidence reflective array filters at 3 GHz. Theory is presented based on a four layer dispersion relation and the impulse model. Experimental results agree well with theory.

INTRODUCTION

Magnetostatic wave (MSW) devices have been developed with signal processing capabilities analogous to SAW [1], but in the 1-20 GHz range with bandwidths approaching 2 GHz. MSW's are slow, dispersive, magnetically dominated waves, which propagate in magnetically biased ferrite materials. High quality, low loss Yttrium Iron Garnet (YIG) films grown on Gadolinium Gallium Garnet substrates by liquid phase epitaxy (LPE) with propagation losses of less than 13 dB/μsec are now available for MSW devices.

Several significant MSW devices have been reported which perform microwave signal processing functions, including oblique incidence refective array filters [2]. Initial studies [3,4] of periodic reflecting structures have shown that periodic etched grooves and metal bar or dot arrays can provide periodic impedance variations in the EPI-YIG yielding filter action. Metal arrays tend to exhibit excessive losses in the metalized YIG region. Etched grooves, when used with magnetostatic forward volume waves (MSFVW), utalized in oblique incidence RAF's, exhibit fringe field coupling to vertical spin modes [5].

In this paper, theoretical and experimental results of the performance of selective Boron ion implantation for oblique incidence MSFVW RAF's are presented.

THEORY

The Dispersion Relation

Magnetostatic Forward Volume Waves were chosen so the obliquely reflected wave would be of the same type as the incident wave (MSFVW), avoiding need for mode conversion mechanisms and allowing the use of a simple impedance discontinuity model for reflection. The isotropic MSFVW wave vector gives equal angle reflections, simplifying bar alignment.

The Polder tensor was derived following the procedure of Wu [6]. A four layer boundary value problem was set up with adjacent implanted and unimplanted YIG layers sandwiched by two dielectric layers, from which the dispersion relation was obtained by requiring the determinant of the six homogeneous magnetic boundary condition equations to be zero for nontrivial solutions. Gilbert loss was included.

Wave Impedance

With MSFVW, a wave impedance can be defined in terms of the transverse field components,

$$Z^{\pm} = \frac{e_z^{\pm}}{h_x^{\pm}} = \pm\frac{\omega u_o}{k} \qquad (1)$$

This follows from Faraday's law, assuming harmonic time variation, negligible field variation with z, and y variation of the form $\exp\pm[-jky]$, and equating the x-components.

In the theory, dispersion relations for the implanted bar structure and the unimplanted gap structure were calculated separately. Sections of these two types were spliced together to form the array, accounting only for impedance discontinuities (transverse field matching). Longitudinal field mismatch should have a negligible effect, since the implanted layer is much thinner than the total YIG thickness.

Ion Implantation

Ion implantation strains the YIG lattice, thus reducing the saturation magnetization and changing the wave impedance. Studies of ion implantation in bubble materials [7], indicate a dose of about 3×10^{15} ions/sq-cm totally randomizes the spins and reduces the magnetization to zero. That work also derived doses and energies for a 0.4 μm deep, double staggered implant with a roughly uniform magnetization profile in the implanted layer (Boron: 3×10^{14} ions/sq-cm @ 70 KeV, 8×10^{14} ions/sq-cm @ 200 KeV). Since the bubble materials studied have about the same density as YIG and the above calculations are based on the same crystallographic orientation used in the MSW work, the doses of that example were scaled to obtain the desired bar reflectivities. Exact data was not available for magnetization change versus dose, so it was linearly approximated between the known end points.

Signal Model

Using the implanted and unimplanted dispersion relations, the reflection coefficient of a bar-gap interface was calculated. For a typical 0.4 μm deep implant, reflection coefficients range from 0.001 to 0.01, and are constant over frequency. Thus, beam refraction at bar-gap boundaries, transmission effects of leading bars, and interbar illumination were neglected, modeling signal flow through the array as a sum of independent reflector contributions. Reflection coefficients for each bar combined reflections from the leading and trailing edges (figure 1).

0149-645X/82/0000-0083 $00.75

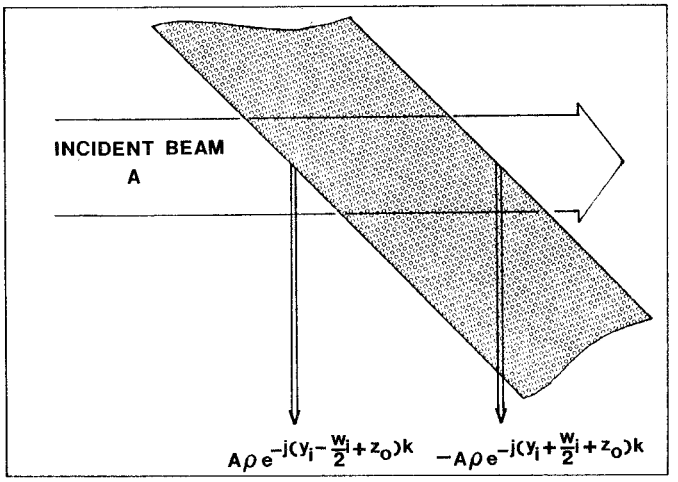

Figure 1. The reflection contribution of the ith bar.

Neglecting beam spreading, power sampling of a bar was modeled as directly proportional to the bar's projection on the input transducer, assuming a uniform wave front across the aperture (aperture much shorter than wavelength in transducer). Summing over N bars gives the array transfer function,

$$T(f)=j2\rho(f)e^{-jkz_o}\sum_{i=1}^{N}\sqrt{l_i/l_t}\,e^{-jky_i}\sin(\frac{kw_i}{2}) \quad (2)$$

where z_o is the distance from the array axis to the output transducer, y_i is the distance from the input transducer to the center of the ith bar, l_i/l_t is the projection of the ith bar onto the input transducer, and w_i is the width of the ith bar. Transducer contributions to the frequency response were modeled after Wu [8].

EXPERIMENT

Experimental Devices

Three MSFVW uniform 20-bar, 90° reflection, transversal filters were fabricated to test the accuracy of the theory for different implant doses. The dose levels, acceleration potentials, and YIG thicknesses are given in Table 1.

Table 1. Implantation Schedule

YIG THICKNESS (UM)	DOSE #1 200 KEV (CM^{-2})	DOSE #2 70 KEV (CM^{-2})	PROJECTED M_{OIMP}/M_O
22.3	6.0×10^{14}	2.3×10^{14}	0.8
23.0	1.2×10^{15}	4.5×10^{14}	0.6
23.0	2.9×10^{15}	1.1×10^{15}	0.0

All implants produce a projected uniform step saturation magnetization change to a 0.4 μm depth. The 45° implanted reflectors were 100 μm wide with 200 μm centers in the propagation direction and a 3 mm transverse aperture. Films were grown by liquid phase epitaxy on a 250 μm gadolinium gallium garnet substrate using a Tolksdorf melt. Thicknesses were chosen nominally the same so that dose level and magnetization effects could be directly compared.

Flipped configuration was used with transducers of 4 μm thick sputtered aluminum on 250 μm thick alumina substrates. A loop input transducer was used to suppress low frequency break through, with a 50 μm wide, 100 μm center spaced, 3 mm aperture filament. The output was a single 7 mm long 50 μm wide shorted bar.

Experiment vs Theory

Theoretical and experimental results are compared on identical scales for the three implant doses in figure 2. These comparisons are summarized in Table 2.

Table 2. Theory / Experiment

M_{OI}/M_O	PEAK I. L. (DB)	SIDELOBE SUPPRESSION (DB)	MAIN LOBE WIDTH (DB)	SIDELOBE WIDTH (DB)
0.8	36.5 / 37	13.3 / 12	42.0 / 40	21.0 / 20
0.6	30.5 / 29	13.3 / 13	42.0 / 45	21.0 / 22
0.0	22.6 / 25	13.3 / NA	42.0 / 50	21.0 / NA

The highest implantation resulted in extensive crystal damage, and it was assumed that the impulse model was not applicable. The two lower dose devices gave good agreement with theory in peak insertion loss, main lobe width, sidelobe suppression, and sidelobe width.

CONCLUSION

This preliminary investigation indicates good agreement between experimental ion implanted MSFVW reflective arrays and a theory based on the magnetostatic approximation and an impulse model. The assumption that a bar-gap interface can be modeled as a simple wave impedance discontinuity is verified. It was shown that ion implanted reflectors work well for MSFVW transversal filters, avoiding the sharp discontinuities associated with etched grooves that cause fringe field coupling to vertical spin waves. A more complete characterization of the effect of implantation dose on saturation magnetization is needed.

ACKNOWLEDGEMENTS

The Air Force Office of Scientific Research is acknowledged for support of this work through grant AFOSR 80-0264. The authors extend special thanks to Texas Instruments for performing the implants and to James M. Zachman for developing the computer graphics used to plot the theoretical results.

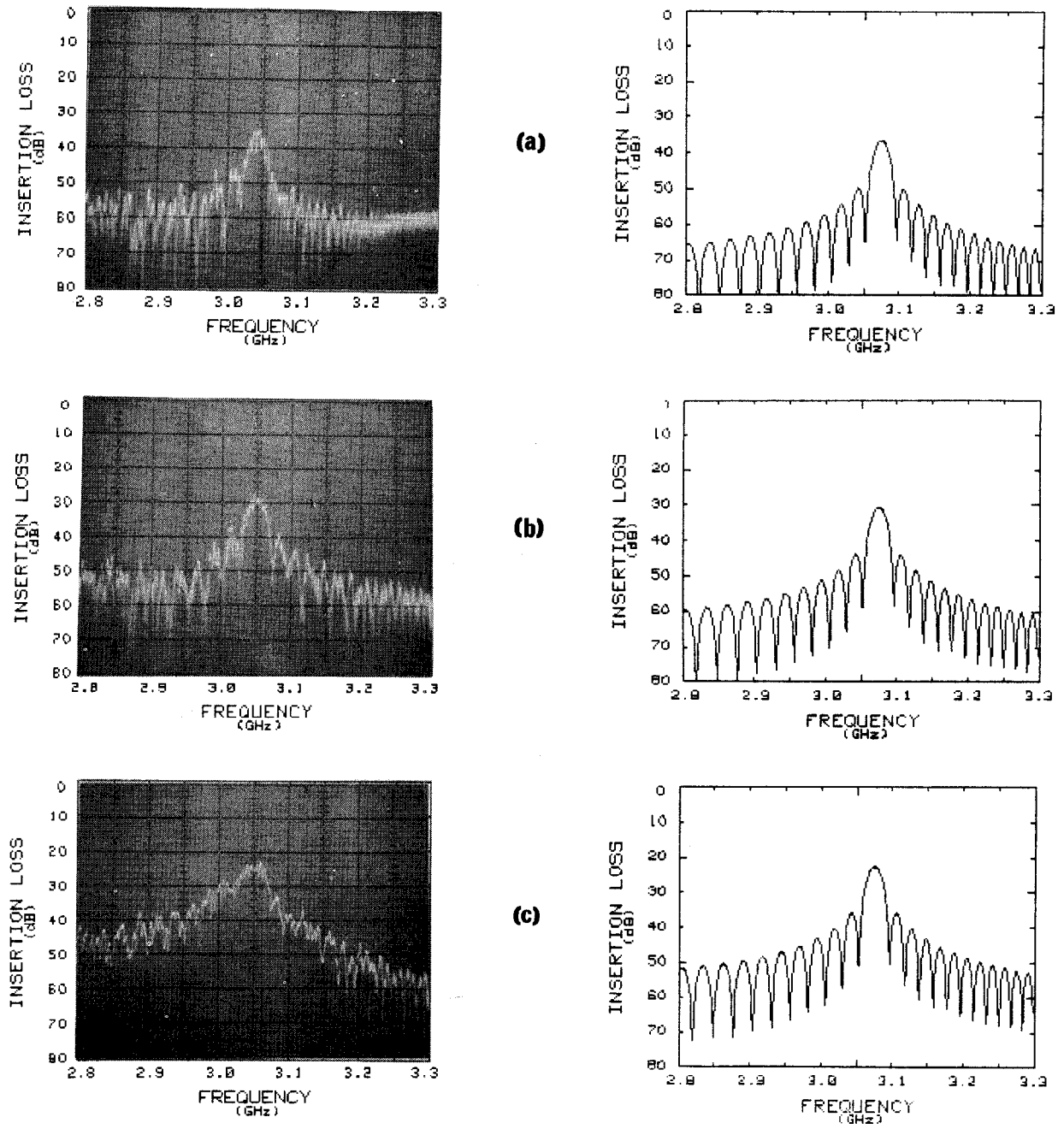

Figure 2. Experiment vs theory (a) Moimp/Mo=0.8, (b) Moimp/Mo=0.6, (b)Moimp/Mo=0.0.

REFERENCES

1. J. M. Owens, R. L. Carter, C. V. Smith, and J. H. Collins, 1980 Ultrasonics Symposium Proceedings, p. 506, IEEE #80CH1602-2.
2. J. M. Owens, C. V. Smith, Jr. and R. L. Carter, 35th Annual Frequency Control Symposium Proceedings, May 1981.
3. C. G. Sykes, J. D. Adam and J. H. Collins Appl. Phys. Lett. 29, 388, (1976).
4. J. M. Owens, et al, IEEE Trans. Mag. 14 388, (1976).
5. R. L. Carter, C. V. Smith, Jr. and J. M. Owens, IEEE Trans. Mag. 16, 1159 (1980).
6. H. J. Wu, Ph.D. Dissertation, The University of Texas at Arlington, Arlington Texas (1978).
7. B. E. MacNeal and V. S. Speriosu, J. Appl. Phys. 52, 3935 (1981).